Journal of Sound and Vibration (2003) **259**(1), 31–43
doi:10.1006/jsvi.2002.5137, available online at http://www.idealibrary.com on IDEAL®

DYNAMIC RESPONSE AND STABILITY ANALYSIS OF AN AUTOMATIC BALL BALANCER FOR A FLEXIBLE ROTOR

J. CHUNG

Department of Mechanical Engineering, Hanyang University, 1271 *Sa*-1-*dong, Ansan, Kyunggi-do* 425-791*, Republic of Korea. E-mail*: *jchung@hanyang.ac.kr*

AND

I. JANG

Department of Mechano-Informatics and Design Engineering, Hongik University, 34 *Sinan-ri, Jochiwon-eup, Yeonki-gun, Chungnam-do* 339-701*, Republic of Korea*

(*Received* 14 *August* 2001, *and in final form* 18 *March* 2002)

Dynamic stability and time responses are studied for an automatic ball balancer of a rotor with a flexible shaft. The Stodola–Green rotor model, of which the shaft is flexible, is selected for analysis. This rotor model is able to include the influence of rigid-body rotations due to the shaft flexibility on dynamic responses. Applying Lagrange's equation to the rotor with the ball balancer, the non-linear equations of motion are derived. Based on the linearized equations, the stability of the ball balancer around the balanced equilibrium position is analyzed. On the other hand, the time responses computed from the non-linear equations are investigated. This study shows that the automatic ball balancer can achieve the balancing of a rotor with a flexible shaft if the system parameters of the balancer satisfy the stability conditions for the balanced equilibrium position.

1. INTRODUCTION

An automatic ball balancer (ABB) is a device to automatically eliminate the variable imbalance of rotating mechanisms. Only one time of balancing is sufficient for a rotor with a fixed amount of imbalance; however, one time of balancing cannot eliminate the imbalance of a rotor with variable imbalance depending on the rotating speed. For this purpose, automatic ball balancers are used to reduce the imbalance in washing machines and optical disk drives such as CD-ROM and DVD drives.

A few studies of ABBs have been reported compared to other balancing topics. The basic research was initiated by Thearl [1, 2], Alexander [3] and Cade [4]. Dynamic analyses for various ball balancers can be found in references [5–7]. Since the previous equations of motion are for non-autonomous systems, these equations have limitations on complete stability analysis. To overcome this drawback, Chung and Ro [8] studied the stability and dynamic behaviour of an ABB for the Jeffcott rotor. They derived the equations of motion for an autonomous system by using the polar co-ordinates instead of the rectangular co-ordinates. Hwang and Chung [9] applied this approach to the analysis of an ABB with double races. However, the previous studies mentioned above dealt with only ball balancers related to the Jeffcott rotor model. The Jeffcott rotor model is inadequate to

0022-460X/02/$35.00

explain the phenomena that arise due to the rigid-body rotation related to shaft flexibility. Therefore, it is needed to study an ABB for a rotor with a flexible shaft.

In this study, the stability and time responses for an ABB are analyzed when the ball balancer is equipped in a rotor with a flexible shaft. Since the Jeffcott rotor model is basically a particle or point-mass representation, this model is inadequate to explain rigid-body characteristics caused by the flexibility of a rotor shaft [10]. Therefore, in order to analyze the dynamics of the balancer for a rotor with a flexible shaft, the Stodola–Green rotor model [11, 12] is adopted instead of the Jeffcott model. Describing the rotor centre with the polar co-ordinates, the non-linear equations of motion for an autonomous system are derived from Lagrange's equation. After a balanced equilibrium position and linearized equations in the neighbourhood of the equilibrium position are obtained by the perturbation method, the stability analysis around the balanced equilibrium position is performed with Routh–Hurwitz criteria and the time responses are also investigated.

2. NON-LINEAR EQUATIONS OF MOTION

The Stodola–Green rotor model with an ABB is shown in Figure 1, where the flexible shaft of length L connects the rigid rotor and the wall. It is assumed that the shaft mass is negligible compared to the rotor mass. The XYZ-co-ordinate system is a space-fixed inertia reference frame and points G and C are the mass centre and centroid of the rotor respectively. Point O may be regarded as projection of the centroid C onto the axis $O'Z$. The ball balancer consists of a circular rotor with a groove containing balls and a damping fluid. The balls move freely in the groove and the rotor spins with angular velocity ω. Since the deflection of the shaft is generally small, it may be assumed that the centroid C moves in the XY-plane. As shown in Figure 2, the centroid C is defined by the polar co-ordinates r and θ. The mass centre G can be defined by eccentricity ε and angle ωt for the given position of the centroid and the angular position of the ball B_i is given by the pitch radius R and angle ϕ_i.

To describe the rigid-body rotations of the rotor with respect to the X- or Y-axis, it is helpful to consider the Euler angles which give the orientation of the rotor-fixed xyz-co-ordinate system relative to the space-fixed XYZ-co-ordinate system. In this study, the Euler angles of $\omega t, \alpha$ and β are used as shown in Figure 2. A rotation through an angle ωt about the Z-axis results in the primed system, i.e., the $x'y'z'$-co-ordinate system. A further

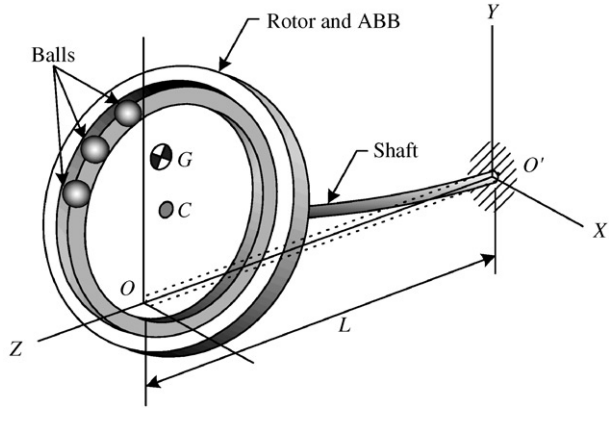

Figure 1. Stodola–Green rotor model with the automatic ball balancer.

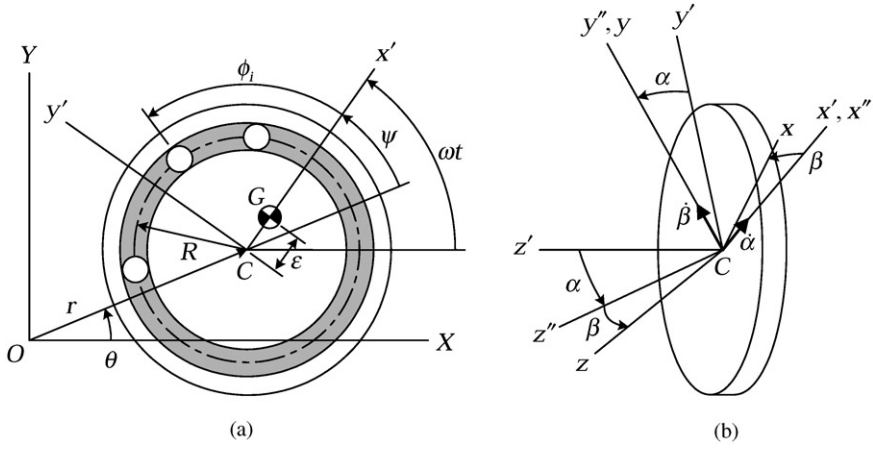

Figure 2. Configuration of an ABB in the Stodola–Green rotor model: (a) the configuration of the balancer after rotation of only ωt, one of the Euler angles; and (b) the configurations of the other Euler angles α and β.

rotation α about the x'-axis puts the rotor into an orientation coincident to the doubled-primed $x''y''z''$-co-ordinate system. Finally, a rotation β about the y''-axis yields the unprimed xyz-co-ordinate system. These co-ordinate transformations can be arranged in the matrix form:

$$\mathbf{x}' = \mathbf{T}_\omega \mathbf{X}, \quad \mathbf{x}'' = \mathbf{T}_\alpha \mathbf{x}', \quad \mathbf{x} = \mathbf{T}_\beta \mathbf{x}'', \tag{1}$$

where

$$\mathbf{T}_\omega = \begin{bmatrix} \cos\omega t & \sin\omega t & 0 \\ -\sin\omega t & \cos\omega t & 0 \\ 0 & 0 & 1 \end{bmatrix}, \quad \mathbf{T}_\alpha = \begin{bmatrix} 1 & 0 & 0 \\ 0 & \cos\alpha & \sin\alpha \\ 0 & -\sin\alpha & \cos\alpha \end{bmatrix}, \quad \mathbf{T}_\beta = \begin{bmatrix} \cos\beta & 0 & -\sin\beta \\ 0 & 1 & 0 \\ \sin\beta & 0 & \cos\beta \end{bmatrix}, \tag{2}$$

$$X = X\hat{\mathbf{I}} + Y\hat{\mathbf{J}} + Z\hat{\mathbf{K}}, \quad \mathbf{x}' = x'\mathbf{i}' + y'\mathbf{j}' + z'\mathbf{k}', \quad \mathbf{x}'' = x''\mathbf{i}'' + y''\mathbf{j}'' + z''\mathbf{k}'', \quad \mathbf{x} = x\mathbf{i} + y\mathbf{j} + z\mathbf{k} \tag{3}$$

in which $\hat{\mathbf{I}}$, $\hat{\mathbf{J}}$ and $\hat{\mathbf{K}}$ are the unit vectors along the X-, Y- and Z-axes; $\mathbf{i}'$, $\mathbf{j}'$and $\mathbf{k}'$ are the unit vectors along the x'-,y'- and z'-axis; $\mathbf{i}, \mathbf{j}$ and $\mathbf{k}$ are the unit vectors along the x-, y- and z-axis respectively.

First, consider the kinetic energy of the rotor system with the ABB. The position vector of the mass centre G can be expressed in the xyz-co-ordinate system by using the rotation matrices, $\mathbf{T}_\omega$, $\mathbf{T}_\alpha$ and $\mathbf{T}_\beta$:

$$\mathbf{r}_G = \mathbf{T}_\beta \mathbf{T}_\alpha \mathbf{T}_\omega \mathbf{r}_{OC/XYZ} + \mathbf{r}_{CG}, \tag{4}$$

where

$$\mathbf{r}_{OC/XYZ} = r(\cos\theta\hat{\mathbf{I}} + \sin\theta\hat{\mathbf{J}}), \quad \mathbf{r}_{CG} = \varepsilon\mathbf{i}. \tag{5}$$

Using a new generalized co-ordinate ψ defined by

$$\psi = \omega t - \theta, \tag{6}$$

the position vector of the mass centre, $\mathbf{r}_G$, and the position vector of the ball B_i, $\mathbf{r}_{Bi}$, can be written as

$$\mathbf{r}_G = [r(\cos\beta\cos\psi - \sin\alpha\sin\beta\sin\psi) + \varepsilon]\mathbf{i} - r\cos\alpha\sin\psi\mathbf{j} + r(\sin\beta\cos\psi + \sin\alpha\cos\beta\sin\psi)\mathbf{k}. \tag{7}$$

$$\mathbf{r}_{Bi} = [r(\cos\beta\cos\psi - \sin\alpha\sin\beta\sin\psi) + R\cos\phi_i]\mathbf{i} + (-r\cos\alpha\sin\psi + R\sin\phi_i)\mathbf{j} + r(\sin\beta\cos\psi + \sin\alpha\cos\beta\sin\psi)\mathbf{k}. \tag{8}$$

When the ball balancer has n balls, the kinetic energy T is given by

$$T = \frac{1}{2}\boldsymbol{\omega}^{\mathrm{T}}\mathbf{J}\boldsymbol{\omega} + \frac{1}{2}M\frac{\mathrm{d}\mathbf{r}_G}{\mathrm{d}t}\cdot\frac{\mathrm{d}\mathbf{r}_G}{\mathrm{d}t} + \frac{1}{2}m\sum_{i=1}^{n}\frac{\mathrm{d}\mathbf{r}_{Bi}}{\mathrm{d}t}\cdot\frac{\mathrm{d}\mathbf{r}_{Bi}}{\mathrm{d}t}. \tag{9}$$

where $\mathbf{J}$ is the inertia matrix and $\boldsymbol{\omega}$ is the angular velocity vector of the rotor:

$$\mathbf{J} = \begin{bmatrix} J & 0 & 0 \\ 0 & J & 0 \\ 0 & 0 & J_z \end{bmatrix}, \tag{10}$$

$$\boldsymbol{\omega} = (-\boldsymbol{\omega}\cos\alpha\sin\beta + \dot{\alpha}\cos\beta)\mathbf{i} + (\boldsymbol{\omega}\sin\alpha + \dot{\beta})\mathbf{j} + (\boldsymbol{\omega}\cos\alpha\cos\beta + \dot{\alpha}\sin\beta)\mathbf{k} \tag{11}$$

in which J is the mass moment of inertia about the x- or y-axis and J_z is the mass moment of inertia about the z-axis.

Neglecting gravity and the torsional and longitudinal deflections of the shaft, the potential energy, or the strain energy, results from the bending deflection of the shaft. As shown in Figure 1, the shaft can be regarded as a cantilever beam, which is fixed at $Z = 0$ and free at $Z = L$. The shaft deflections in the X and Y directions at $Z = L$, D_X and D_Y, are given by

$$D_X = r\cos\theta, \quad D_Y = r\sin\theta. \tag{12}$$

For the given rotation angles α and β, the rotation angles about the X- and Y-axis, Φ_X and Φ_Y, are given by

$$\Phi_X = \alpha\cos\omega t - \beta\cos\alpha\sin\omega t, \quad \Phi_Y = \alpha\sin\omega t + \beta\cos\alpha\cos\omega t. \tag{13}$$

Since the deflection and slope at $Z = L$ in the ZX-plane are D_X and Φ_Y while those in the ZY-plane are D_Y and $-\Phi_X$, the deflection curves of the shaft in the ZX- and ZY-planes, δ_X and δ_Y, can be expressed as

$$\delta_X = \frac{3D_X - L\Phi_Y}{L^2}Z^2 - \frac{2D_X - L\Phi_Y}{L^3}Z^3, \quad \delta_Y = \frac{3D_Y + L\Phi_X}{L^2}Z^2 - \frac{2D_Y + L\Phi_X}{L^3}Z^3. \tag{14}$$

In this case, the strain energy V due to the shaft bending is

$$V = \frac{1}{2}EI\int_0^L \left[\left(\frac{\partial^2\delta_X}{\partial Z^2}\right)^2 + \left(\frac{\partial^2\delta_Y}{\partial Z^2}\right)^2\right]\mathrm{d}Z, \tag{15}$$

where E is Young's modulus and I is the area moment of inertia of the shaft cross-section.

On the other hand, Rayleigh's dissipation function F can be represented by

$$F = \frac{1}{2}c_t(\dot{r}^2 + r^2\dot{\theta}^2) + \frac{1}{2}c_r(\dot{\alpha}^2 + \dot{\beta}^2) + \frac{1}{2}D\sum_{i=1}^{n}\dot{\phi}_i^2, \tag{16}$$

where c_t is the equivalent damping coefficient for translation, c_r is the equivalent damping coefficient for rotation, and D is the viscous drag coefficient of the ball in the damping fluid. It is assumed that the balls have the same viscous drag coefficient D.

The equations of motion for the ABB are derived from Lagrange's equation given by

$$\frac{\mathrm{d}}{\mathrm{d}t}\left(\frac{\partial T}{\partial \dot{q}_k}\right) - \frac{\partial T}{\partial q_k} + \frac{\partial V}{\partial q_k} + \frac{\partial F}{\partial \dot{q}_k} = 0, \tag{17}$$

where q_k are the generalized co-ordinates. For the given system, the generalized co-ordinates are r, ψ, α, β and $\phi_i (i = 1, 2, \ldots, n)$; therefore, the dynamic behaviour of the balancer is governed by $n + 4$ independent equations of motion. Substitution of equations (9), (15) and (16) into equation (17) yields the equations of motion. Since r, α, β and ε are small, the products of these parameters are negligible. Under the assumption that r, α, β and ε are small, the equations of motion are simplified to

$$(M+nm)[\ddot{r} - r(\omega - \dot{\psi})^2] + c_t\dot{r} + \frac{12EI}{L^3}r - \frac{6EI}{L^2}\alpha\sin\psi - \frac{6EI}{L^2}\beta\cos\psi$$

$$- mR\sum_{i=1}^{n}[\ddot{\phi}_i\sin(\phi_i+\psi) + (\dot{\phi}_i+\omega)^2\cos(\phi_i+\psi)] = M\varepsilon\omega^2\cos\psi, \tag{18}$$

$$(M+nm)[r\ddot{\psi} - 2\dot{r}(\omega - \dot{\psi})] - c_t r(\omega - \dot{\psi}) - \frac{6EI}{L^2}\alpha\cos\psi + \frac{6EI}{L^2}\beta\sin\psi$$

$$- mR\sum_{i=1}^{n}[\ddot{\phi}_i\cos(\phi_i+\psi) - (\dot{\phi}_i+\omega)^2\sin(\phi_i+\psi)] = -M\varepsilon\omega^2\sin\psi, \tag{19}$$

$$\left(J + mR^2\sum_{i=1}^{n}\sin^2\phi_i\right)\ddot{\alpha} - mR^2\ddot{\beta}\sum_{i=1}^{n}\cos\phi_i\sin\phi_i$$

$$+ \left(c_r + 2mR^2\sum_{i=1}^{n}\dot{\phi}_i\cos\phi_i\sin\phi_i\right)\dot{\alpha} + \left[(J_z - 2J)\omega + 2mR^2\sum_{i=1}^{n}\dot{\phi}_i\sin^2\phi_i\right]\dot{\beta}$$

$$- \frac{6EI}{L^2}r\sin\psi + \left[\frac{4EI}{L} + (J_z - J)\omega^2 + mR^2\sum_{i=1}^{n}(2\omega\dot{\phi}_i + \omega^2)\sin^2\phi_i\right]\alpha$$

$$+ mR^2\beta\sum_{i=1}^{n}[\ddot{\phi}_i - (2\omega\dot{\phi}_i + \omega^2)\cos\phi_i\sin\phi_i] = 0, \tag{20}$$

$$- mR^2\ddot{\alpha}\sum_{i=1}^{n}\cos\phi_i\sin\phi_i + \left(J + mR^2\sum_{i=1}^{n}\cos^2\phi_i\right)\ddot{\beta}$$

$$- \left[(J_z - 2J)\omega + 2mR^2\sum_{i=1}^{n}\dot{\phi}_i\cos^2\phi_i\right]\dot{\alpha} + \left(c_r - 2mR^2\sum_{i=1}^{n}\dot{\phi}_i\cos\phi_i\sin\phi_i\right)\dot{\beta}$$

$$- \frac{6EI}{L^2}r\cos\psi - mR^2\alpha\sum_{i=1}^{n}(2\omega\dot{\phi}_i + \omega^2)\cos\phi_i\sin\phi_i$$

$$+ \left[\frac{4EI}{L} + (J_z - J)\omega^2 + mR^2\sum_{i=1}^{n}(2\omega\dot{\phi}_i + \omega^2)\cos^2\phi_i\right]\beta = 0 \tag{21}$$

$$m R^2 \ddot{\phi}_i + D\dot{\phi}_i - mR[\ddot{r} - r(\omega - \dot{\psi})^2]\sin(\phi_i + \psi) + mR[-r\ddot{\psi}$$

$$+ 2\dot{r}(\omega - \dot{\psi})]\cos(\phi_i + \psi) = 0, \quad i = 1, 2, \ldots, n. \tag{22}$$

It is noted that the equations of motion given by equations (18)–(22) are non-linear because ψ and ϕ_i are not small while r, α and β are small.

3. BALANCED POSITION AND LINEARIZED EQUATIONS

The perturbation method is used to obtain equilibrium positions and linearized perturbation equations of motion in the neighbourhood of the equilibrium positions. The generalized co-ordinates r, ψ, α, β and ϕ_i can be represented by

$$r = r^* + \Delta r, \quad \psi = \psi^* + \Delta\psi, \quad \alpha = \alpha^* + \Delta\alpha, \quad \beta = \beta^* + \Delta\beta, \quad \phi_i = \phi_i^* + \Delta\phi_i, \tag{23}$$

where r^*, ψ^*, α^*, β^* and ϕ_i^* are the co-ordinates for an equilibrium position and Δr, $\Delta\psi$, $\Delta\alpha$, $\Delta\beta$ and $\Delta\phi_i$ are the small perturbations of the generalized co-ordinates in the neighbourhood of the equilibrium position.

As discussed in reference [4], the equilibrium positions may be classified into two cases: the balanced and unbalanced cases, which correspond to $r^* = 0$ and $\neq 0$ respectively. Since the balanced equilibrium position of $r^* = 0$ is important from a practical point of view, only the equilibrium position corresponding to $r^* = 0$ and the linearized equations in the neighbourhood of theses equilibrium positions are considered in this study. Substitution of equations (23) into equations (18)–(22) results in the balanced equilibrium positions and the linearized equations about the balanced equilibrium position. The balanced equilibrium positions are given by

$$r^* = \alpha^* = \beta^* = 0, \quad \sum_{i=1}^{n} \cos\phi_i^* = -\frac{M\varepsilon}{mR}, \quad \sum_{i=1}^{n} \sin\phi_i^* = 0. \tag{24}$$

It should be pointed out that ψ^* cannot be defined for the balanced equilibrium positions. For simplicity, deleting Δ from Δr, $\Delta\psi$, $\Delta\alpha$, $\Delta\beta$ and $\Delta\phi_i$, the linearized equations of motion are written as

$$(M + nm)\ddot{r} + c_t\dot{r} + \left[\frac{12EI}{L^3} - (M + nm)\omega^2\right] r - \frac{6EI}{L^2}\alpha\sin\psi^*$$

$$- \frac{6EI}{L^2}\beta\cos\psi^* - mR\sum_{i=1}^{n}[\ddot{\phi}_i\sin(\phi_i^* + \psi^*)$$

$$+ 2\omega\dot{\phi}_i\cos(\phi_i^* + \psi^*) - \omega^2\phi_i\sin(\phi_i^* + \psi^*)] = 0 \tag{25}$$

$$-2(M + nm)\omega\dot{r} - c_t\omega r - \frac{6EI}{L^2}\alpha\cos\psi^* + \frac{6EI}{L^2}\beta\sin\psi^* - mR\sum_{i=1}^{n}[\ddot{\phi}_i\cos(\phi_i^* + \psi^*)$$

$$- 2\omega\dot{\phi}_i\sin(\phi_i^* + \psi^*) - \omega^2\phi_i\cos(\phi_i^* + \psi^*)] = 0, \tag{26}$$

$$\left(J + mR^2\sum_{i=1}^{n}\sin^2\phi_i^*\right)\ddot{\alpha} - mR^2\ddot{\beta}\sum_{i=1}^{n}\cos\phi_i^*\sin\phi_i^* + c_r\dot{\alpha} + (J_z - 2J)\omega\dot{\beta} - \frac{6EI}{L^2}r\sin\psi^*$$

$$+ \left[\frac{4EI}{L} + (J_z - J)\omega^2 + mR^2\omega^2\sum_{i=1}^{n}\sin^2\phi_i^*\right]\alpha - mR^2\omega^2\beta\sum_{i=1}^{n}\cos\phi_i^*\sin\phi_i^* = 0, \tag{27}$$

$$-mR^2\ddot{\alpha}\sum_{i=1}^{n}\cos\phi_i^*\sin\phi_i^* + \left(J + mR^2\sum_{i=1}^{n}\cos^2\phi_i^*\right)\ddot{\beta} - (J_z - 2J)\omega\dot{\alpha} + c_r\dot{\beta} - \frac{6EI}{L^2}r\cos\psi^*$$

$$-mR^2\omega^2\alpha\sum_{i=1}^{n}\cos\phi_i^*\sin\phi_i^* + \left[\frac{4EI}{L} + (J_z - J)\omega^2 + mR^2\omega^2\sum_{i=1}^{n}\cos^2\phi_i^*\right]\beta = 0, \tag{28}$$

$$mR^2\ddot{\phi}_i + D\dot{\phi}_i - mR[\ddot{r}\sin(\phi_i^* + \psi^*) - 2\omega\dot{r}\cos(\phi_i^* + \psi^*) - \omega^2 r\sin(\phi_i^* + \psi^*)]$$

$$= 0, \quad i = 1, 2, \ldots, n \tag{29}$$

4. STABILITY ANALYSIS

The stability of the ABB is analyzed with the linearized equations of motion in the neighbourhood of the balanced equilibrium position. For simplicity of the stability analysis, it is assumed that the number of balls is two, i.e., $n = 2$. When the ball balancer has two balls, the steady state solutions can be classified into two: one is for the balanced equilibrium position and the other is for the unbalanced equilibrium position. Since the unbalanced equilibrium position is not practically important compared to the balanced position, the stability analysis in the neighbourhood of the unbalanced position is omitted from this paper. The mass moments of inertia, J and J_z, are given by

$$J = \tfrac{1}{4}MR^2, \quad J_z = \tfrac{1}{2}MR^2 \tag{30}$$

and the balanced equilibrium position is represented by

$$r^* = \alpha^* = \beta^* = 0, \quad \phi_1^* = -\phi_2^* = -\tan^{-1}\sqrt{(2mR/M\varepsilon)^2 - 1}. \tag{31}$$

It is noted that the value of ψ^* is not defined when $r^* = 0$. In order to analyze the stability in the neighbourhood of the balanced equilibrium position, small perturbations of the generalized co-ordinates from the balanced position can be written as

$$r = X_r e^{\lambda t}, \quad \alpha = X_\alpha e^{\lambda t}, \quad \beta = X_\beta e^{\lambda t}, \quad \phi_1 = X_{\phi 1} e^{\lambda t}, \quad \phi_2 = X_{\phi 2} e^{\lambda t}, \tag{32}$$

where λ is a characteristic value or an eigenvalue. Substituting equations (31) and (32) into equations (25)–(29) and using the identity equation

$$\cos^2\psi^* + \sin^2\psi^* = 1, \tag{33}$$

the condition that equations (32) have non-trivial solutions can be expressed as the characteristic equation given as

$$\sum_{k=0}^{12} c_k\lambda^k = 0, \tag{34}$$

where the coefficients c_k $(k = 0, 1, \ldots, 12)$ are functions of ω, $M, m, R, L, \varepsilon, E, I, D$, c_t and c_r. Since c_k are complicated functions of the above system parameters, the explicit expressions are omitted from this paper.

The Routh–Hurwitz criteria are used to investigate the stability of the ABB. If all the eigenvalues, namely, the roots of equation (34) have negative real parts, the ball balancer is asymptotically stable. The Routh–Hurwitz criteria provide the necessary and sufficient conditions for the real parts of all roots to be negative. For convenience of discussion, the

following parameters are introduced:

$$\omega_0 = \sqrt{\frac{12EI}{ML^3}}, \quad \zeta_t = \frac{c_t}{4}\sqrt{\frac{L^3}{3MEI}}, \quad \zeta_r = \frac{c_r}{4}\sqrt{\frac{L}{JEI}}, \tag{35}$$

where ω_0 is the reference frequency; ζ_t and ζ_r are dimensionless damping factors for translation and rotation. The stability of the balancer are studied for the variations of the non-dimensional system parameters such as ω/ω_0, m/M, ε/R, $D/mR^2\omega_0$, ζ_t and ζ_r. The description of the stability for the variations of all the system parameters is impossible, so in this study the stability is analyzed with the variations of a pair of parameters, that is, ω/ω_0 versus m/M, ω/ω_0 versus ε/R, ω/ω_0 versus $D/mR^2\omega_0$, ω/ω_0 versus ζ_t, and ω/ω_0 versus ζ_r. The non-dimensional parameters for all the stability analyses are given by $L/R = 1$ and $m/M = \varepsilon/R = D/mR^2\omega_0 = \zeta_t = \zeta_r = 0{\cdot}01$.

First, consider the stability of the automatic ball balancer in the neighbourhood of the balanced equilibrium position for the variations of the rotating speed, the ball mass and the eccentricity. Figure 3(a) shows the stable region or the balancing region for the variation of ω/ω_0 versus m/M while Figure 3(b) shows the stable region for the variation of ω/ω_0 versus ε/R. The straight boundaries in Figures 3(a) and (b) are related to the condition given by

$$2\frac{m}{M} \geqslant \frac{\varepsilon}{R}, \tag{36}$$

which implies that the mass of two balls should be large enough to cover the imbalance of the rotor. It is also shown in equation (31) that the ball position cannot be defined if the inequality equation of equation (36) is not satisfied. Denoting the natural frequencies of the rotor without balls by ω_1 and ω_2, these natural frequencies can be obtained from

$$\begin{bmatrix} M & 0 \\ 0 & J \end{bmatrix} \begin{Bmatrix} \ddot{r} \\ \ddot{\alpha} \end{Bmatrix} + \frac{2EI}{L^3} \begin{bmatrix} 6 & -3L \\ -3L & 2L^3 \end{bmatrix} \begin{Bmatrix} r \\ \alpha \end{Bmatrix} = \begin{Bmatrix} 0 \\ 0 \end{Bmatrix}. \tag{37}$$

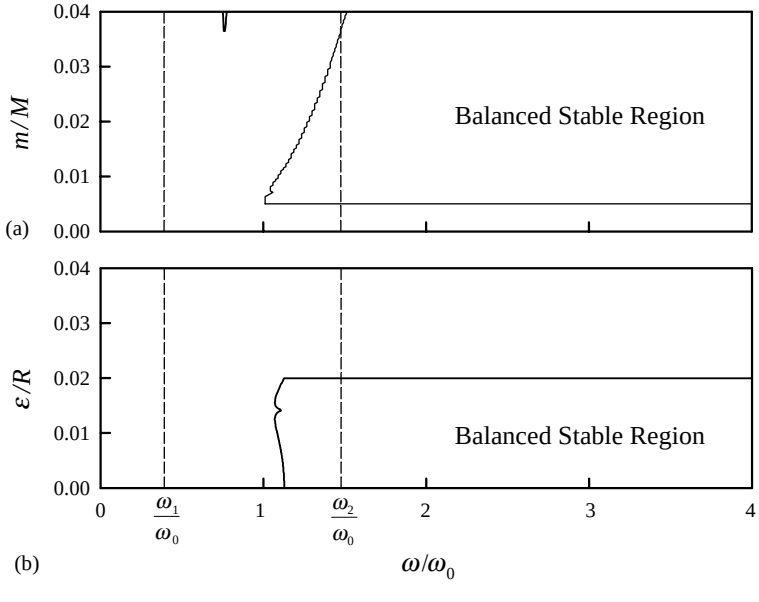

Figure 3. Stability in the neighbourhood of the balanced equilibrium position for the variations of the rotating speed, the ball mass and the eccentricity: (a) ω/ω_0 versus m/M; and (b) ω/ω_0 versus ε/R.

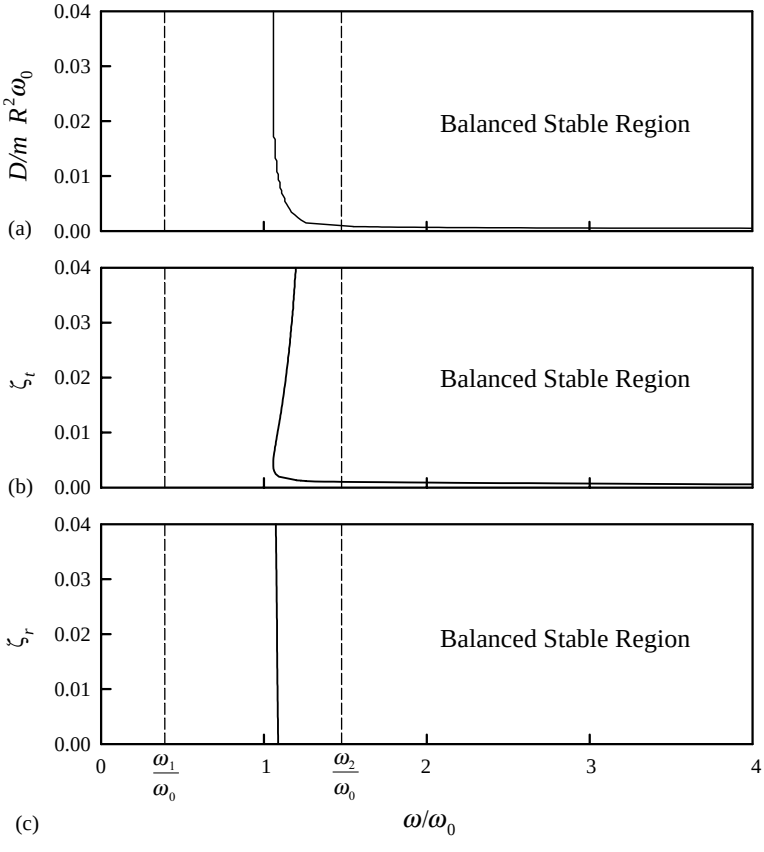

Figure 4. Stability in the neighbourhood of the balanced equilibrium position for the variations of the rotating speed and the damping factors: (a) ω/ω_0 versus $D/mR^2\omega_0$; (b) ω/ω_0 versus ζ_t; and (c) ω/ω_0 versus ζ_r.

It is interesting that the stability in the neighbourhood of the balanced equilibrium position is guaranteed when the rotating speed ω is greater than the first natural frequency ω_1 of the rotor. However, it seems that the second natural frequency ω_2 is irrelevant to the stability of the rotor.

Next, the effects of the dissipation mechanisms on stability are analyzed. Figures 4(a) and (b) show that the ABB is not able to achieve the balance of the rotor if $D = 0$ or $\zeta_t = 0$. This means that the fluid damping D and the dissipation for translation ζ_t are crucial factors for balancing. However, Figure 4(c) demonstrates that the automatic balancer is stable about the balanced equilibrium position even when $\zeta_r = 0$. In other words, the balancer without damping for rotation can obtain balance.

5. TIME RESPONSES

Time responses of the ABB are investigated to verify the stability of the ball balancer and to analyze the dynamic behaviour. From the non-linear equations of motion given by equations (18)–(22), the time responses are computed by the generalized-α time integration method [13]. When the ball balancer has two balls, i.e., $n = 2$, the non-linear equations (18)–(22) may be expressed by the following matrix–vector equation:

$$\mathbf{M}(\mathbf{x})\ddot{\mathbf{x}} + \mathbf{N}(\dot{\mathbf{x}}, \mathbf{x}) = \mathbf{0}, \tag{38}$$

where **M** is the mass matrix, **N** is the non-linear internal force vector, and **x** is the displacement vector:

$$\mathbf{x} = \{r, \psi, \alpha, \beta, \phi_1, \phi_2\}^{\mathrm{T}}. \tag{39}$$

Note that the mass matrix **M** is a function of the displacement vector **x** while the internal force vector **N** is a function of the displacement vector **x** and the velocity vector $\dot{\mathbf{x}}$. The material properties and dimensions for computation of time responses are given by $R = 0{\cdot}1\,\mathrm{m}$, $M = 1\,\mathrm{kg}$, $m = 0{\cdot}001\,\mathrm{kg}$, $EI = 10\,\mathrm{Nm}^2$, $L/R = 1$ and $m/M = \varepsilon/R = D/mR^2\omega_0 = \zeta_t = \zeta_r = 0{\cdot}01$. The mass moments of inertia, J and J_z, are given by equations (30). The procedure to obtain the time responses by using the generalized-α method can be found in reference [4].

Time responses are computed for the cases of $\omega/\omega_0 = 0{\cdot}5$, 1 and 3. The initial conditions are given as $r(0) = 0{\cdot}001\,\mathrm{m}$, $\psi(0) = 0^\circ$, $\alpha(0) = 18^\circ$, $\beta(0) = 18^\circ$, $\phi_1(0) = 45^\circ$ and

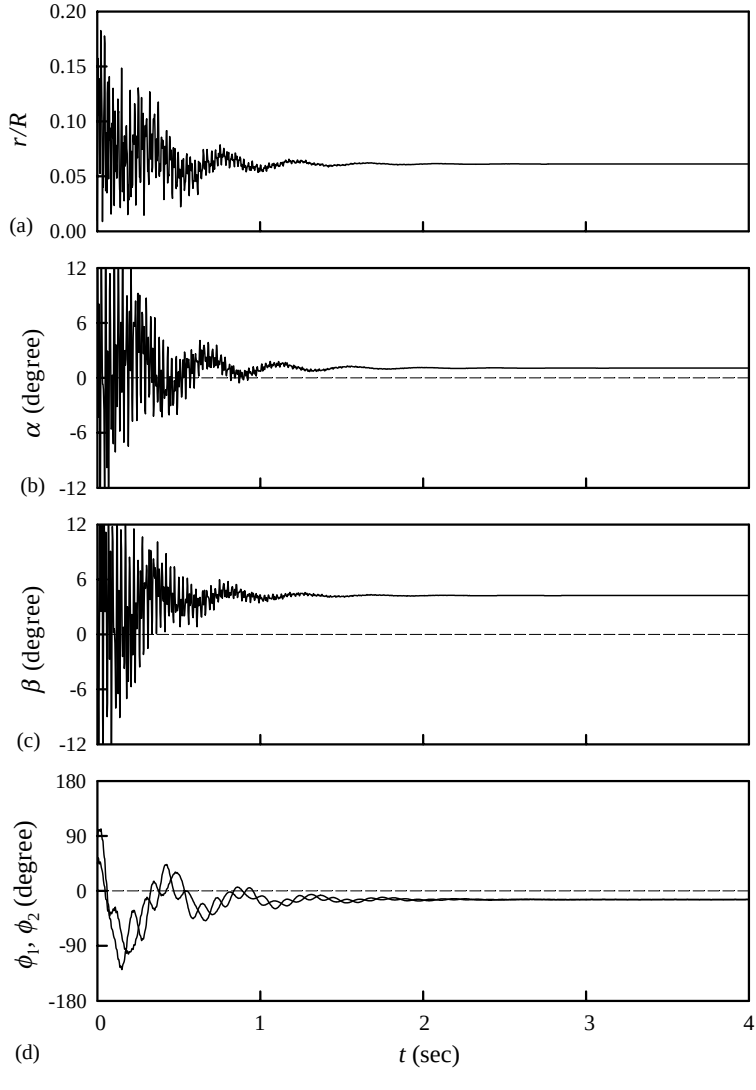

Figure 5. Time responses of the automatic ball balancer when $\omega/\omega_0 = 0.5$: (a) the radial displacement r; (b) the rotation angle α; (c) the rotation angle β; and (d) the ball positions ϕ_1 and ϕ_2.

$\phi_2(0) = 90^\circ$. Figures 3 and 4 show that the rotating speeds of $\omega/\omega_0 = 0{\cdot}5$ and 1 are in the unstable region for the balanced equilibrium position if the balancer has the system parameters given above. On the other hand, it is observed that the speed of $\omega/\omega_0 = 3$ is in the stable region. Time responses of the ABB, when $\omega/\omega_0 = 0{\cdot}5$, are presented in Figure 5. This figure demonstrates that, as time increases, the non-dimensional radial displacement, the rotation angles and the ball positions converge to $r/R = 0{\cdot}0612$, $\alpha = 1{\cdot}0703^\circ, \beta = 4{\cdot}2412^\circ$ and $\phi_1 = \phi_2 = -14{\cdot}1424^\circ$ respectively. Therefore, the ball balancer does not perform the balancing of the rotor that may be expressed by $r = \alpha = \beta = 0$. Figure 6 demonstrates that when $\omega/\omega_0 = 1$ the ball balancer is also unstable in the neighbourhood of the balanced equilibrium position. In Figure 6, the radial displacement, the rotation angles and the ball positions are varied continually with time so that they do not have the converged values. However, when the ball balancer is in the stable region for the balanced

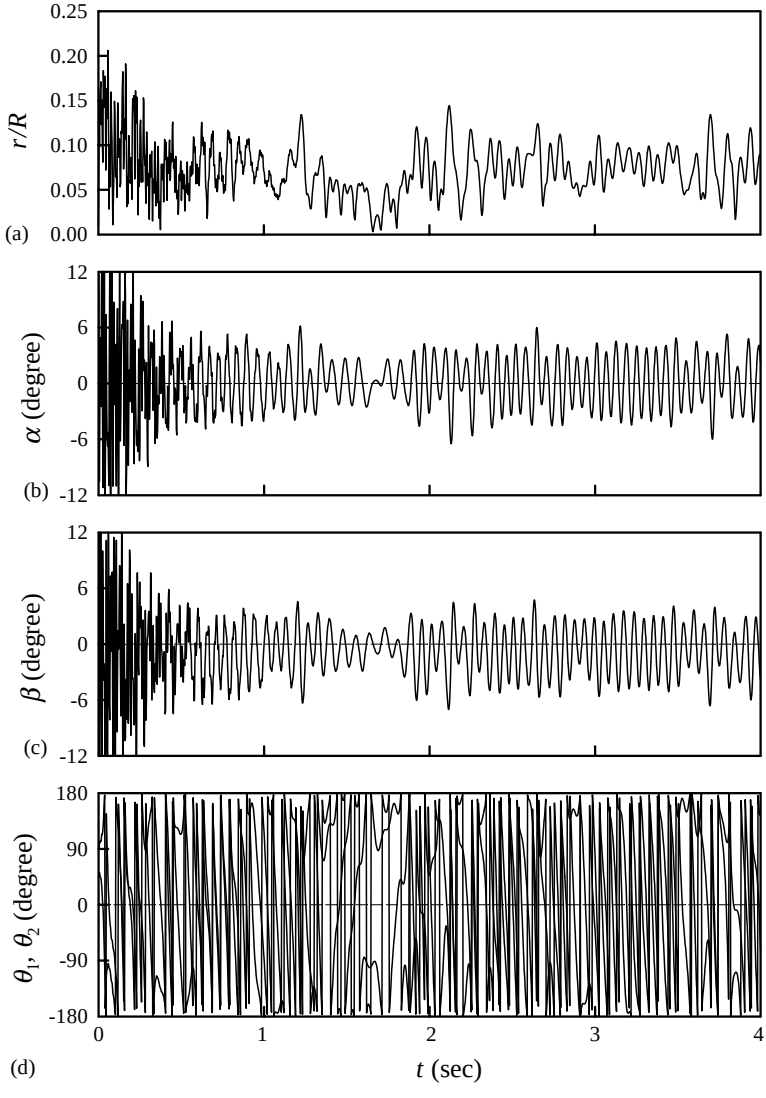

Figure 6. Time responses of the automatic ball balancer when $\omega/\omega_0 = 1$: (a) the radial displacement r; (b) the rotation angle α; (c) the rotation angle β; and (d) the ball positions ϕ_1 and ϕ_2.

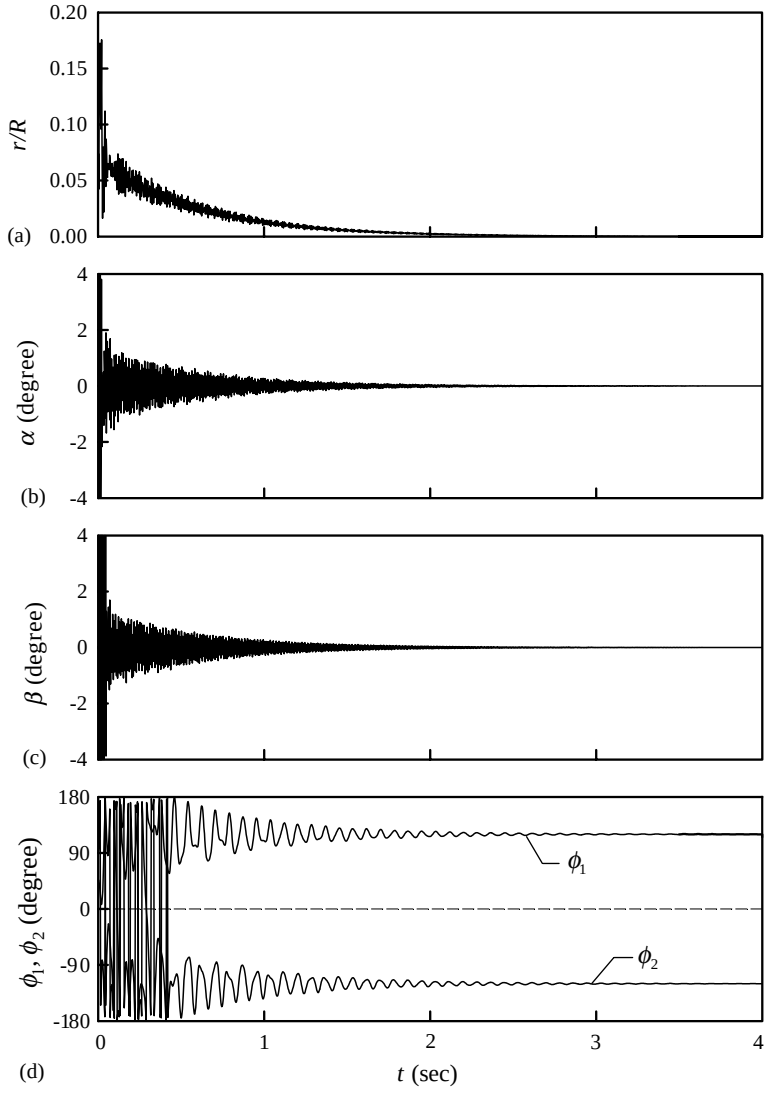

Figure 7. Time responses of the automatic ball balancer when $\omega/\omega_0 = 3$: (a) the radial displacement r; (b) the rotation angle α; (c) the rotation angle β; and (d) the ball positions ϕ_1 and ϕ_2.

equilibrium position, e.g., when $\omega/\omega_0 = 3$, the balancer achieves the balancing of the rotor. In this case, the radial displacement and the rotation angles converge to zero, i.e., $r = \alpha = \beta = 0$, as shown in Figures 7(a), (b) and (c). Figure 7(d) demonstrates that the converged values for the ball positions are $\phi_1 = 120^\circ$ and $\phi_2 = -120^\circ$, which can be obtained from equations (31) and satisfy equations (24). This means that the balancer is not only in static equilibrium but also in dynamic equilibrium.

6. CONCLUSIONS

In this paper, dynamic stability and responses are analyzed for an automatic ball balancer of a rotor with a flexible shaft. To consider rigid-body rotations due to shaft flexibility, this study adopts the Stodola–Green rotor model instead of the Jeffcott rotor

model. With the ball balancer of the Stodola–Green rotor, the non-linear equations of motion are newly derived, which are for an autonomous system. Applying the perturbation method to these equations, a balanced equilibrium position and linearized equations in the neighbourhood of the equilibrium position are obtained.

Based on the linearized equations, in the neighbourhood of the balanced equilibrium position, the stability analysis is performed by using the Routh–Hurwitz criteria. On the other hand, time responses are computed from the non-linear equations of motion and they are investigated. The results of this study may be summarized as follows.

(1) The automatic ball balancer can achieve the balancing of the Stodola–Green rotor as well as the Jeffcott rotor.
(2) The balancing can be obtained only in the case in which the system parameters are in the stability region for the balanced equilibrium position.
(3) To obtain the balancing, the rotating speed should be greater than the first natural frequency; however, it may be less than the second natural frequency.
(4) The fluid damping D and the dissipation for translation c_t are essential to obtain balancing, but the dissipation for rotation c_r is not.
(5) When the ball balancer enables a rotor to be balanced, not only the radial displacement r but also the rotation angles α and β converge to zero with time.

REFERENCES

1. E. L. Thearle 1950 *Machine Design* **22**, 119–124. Automatic dynamic balancers (Part 1. leblanc balancer).
2. E. L. Thearle 1950 *Machine Design* **22**, 103–106. Automatic dynamic balancers (Part 2. ring, pendulum, ball balancers).
3. J. D. Alexander 1964 *Proceedings of 2nd Southeastern Conference* vol. 2, 415–426. An automatic dynamic balancer.
4. J. W. Cade 1965 *Design News*, 234–239. Self-compensating balancing in rotating mechanisms.
5. J. Lee and W. K. Van Moorhem 1996 *American Society of Mechanical Engineers Journal of Dynamic Systems, Measurement, and Control* **118**, 468–475. Analytical and experimental analysis of a self-compensating dynamic balancer in a rotating mechanism.
6. M. Tadeusz 1988 *Mechanism and Machine Theory* **23**, 71–78. Position errors occurrence in self balancers used on rigid rotors of rotating machinery.
7. C. Rajalingham and S. Rakheja 1998 *Journal of Sound and Vibration* **217**, 453–466. Whirl suppression in hand-held power tool rotors using guided rolling balancers.
8. J. Chung and D. S. Ro 1999 *Journal of Sound and Vibration* **228**, 1035–1056. Dynamic analysis of an automatic dynamic balancer for rotating mechanisms.
9. C. H. Hwang and J. Chung 1999 *JSME International Journal* **42**, 265–272. Dynamic analysis of an automatic ball balancer with double races.
10. D. Childs 1993 Turbomachinery Rotordynamics: Phenomena, Modeling, and Analysis. New York: John Wiley & Sons, Inc.
11. A. Stodola 1927 *Steam and Gas Turbines.* New York: McGraw-Hill.
12. R. Green 1948 *American Society of Mechanical Engineers Journal of Applied Mechanics* **15**, 369–376. Gyroscopic effects of the critical speeds of a flexible rotors.
13. J. Chung and G. M. Hulbert 1993 *American Society of Mechanical Engineers Journal of Applied Mechanics* **60**, 371–375. A time integration algorithm for structural dynamics with improved numerical dissipation: the generalized-α method.